ATMOSPHERIC AND OCEANIC SCIENCE LETTERS, 2015, VOL. 8, NO. 2, 88–94

# Improving Simulation of the Terrestrial Carbon Cycle of China in Version 4.5 of the Community Land Model Using a Revised $V_{cmax}$ Scheme

WANG Yuan-Yuan[1,2], XIE Zheng-Hui[1*], JIA Bing-Hao[1], and YU Yan[3]

[1] *State Key Laboratory of Numerical Modeling for Atmospheric Sciences and Geophysical Fluid Dynamics (LASG), Institute of Atmospheric Physics, Chinese Academy of Sciences, Beijing 100029, China*
[2] *University of Chinese Academy of Sciences, Beijing 100049, China*
[3] *Zhejiang Institute of Meteorological Sciences, Hangzhou 310017, China*

Received 8 December 2014; revised 16 February 2015; accepted 16 February 2015; published 16 March 2015

**Abstract** The maximum rate of carboxylation ($V_{cmax}$) is a key photosynthetic parameter for gross primary production (GPP) estimation in terrestrial biosphere models. A set of observation-based $V_{cmax}$ values, which take the nitrogen limitation on photosynthetic rates into consideration, are used in version 4.5 of the Community Land Model (CLM4.5). However, CLM4.5 with carbon-nitrogen (CN) biogeochemistry (CLM4.5-CN) still uses an independent decay coefficient for nitrogen after the photosynthesis calculation. This means that the nitrogen limitation on the carbon cycle is accounted for twice when CN biogeochemistry is active. Therefore, to avoid this double nitrogen down-regulation in CLM4.5-CN, the original $V_{cmax}$ scheme is revised with a new one that only accounts for the transition between $V_{cmax}$ and its potential value (without nitrogen limitation). Compared to flux tower-based observations, the new $V_{cmax}$ scheme reduces the root-mean-square error (RMSE) in GPP for mainland China by 13.7 g C m$^{-2}$ yr$^{-1}$, with a larger decrease over humid areas (39.2 g C m$^{-2}$ yr$^{-1}$). Moreover, net primary production and leaf area index are also improved, with reductions in RMSE by 0.8% and 11.5%, respectively.

**Keywords:** CLM4.5, $V_{cmax}$, gross primary production, net primary production, leaf area index

**Citation:** Wang, Y.-Y., Z.-H. Xie, B.-H. Jia, et al., 2015: Improving simulation of the terrestrial carbon cycle of China in version 4.5 of the Community Land Model using a revised $V_{cmax}$ scheme, *Atmos. Oceanic Sci. Lett.*, **8**, 88–94, doi:10.3878/AOSL20140090.

## 1 Introduction

The terrestrial carbon cycle is an important aspect of global change, and modeling it has been an effective tool in understanding its processes. Gross primary production (GPP) is a key component of the terrestrial carbon balance, which needs to be simulated as accurately as possible to ensure the most reliable values of the latter's simulated fluxes and biomass, such as net primary production (NPP) and leaf area index (LAI) (Schaefer et al., 2012). Most terrestrial biosphere models commonly use a variant of the Farquhar et al. (1980) photosynthesis model coupled to the Ball-Berry stomatal conductance model (Collatz et al., 1991). A key term in the equations for the calculation of GPP is the photosynthetic parameter $V_{cmax}$, which describes the maximum rate of carboxylation by the photosynthetic enzyme Rubisco at leaf-level (Bonan et al., 2012). Some studies suggest that model structural errors could be compensated by parameter adjustment, and this may explain the lack of consensus in values of $V_{cmax}$ used in different photosynthesis models (Bonan et al., 2011, 2012; Chen et al., 2011).

The photosynthetic parameter values of $V_{cmax}$ used in version 4.5 of the Community Land Model (CLM4.5) were obtained from the results of Kattge et al. (2009), which were based on a meta-analysis of photosynthetic measurements extrapolated to field vegetation, using observed foliage content, and those values are included in the TRY global database of plant traits (Kattge et al., 2011; see http://www.try-db.org). The parameters already reflect nitrogen limitation on photosynthetic rates. However, for CLM4.5 with carbon-nitrogen (CN) biogeochemistry (denoted as CLM4.5-CN), the nitrogen-induced reduction of GPP is applied after the photosynthesis calculation and is independent of $V_{cmax}$, which means that the potential $V_{cmax25}^{opt}$ (without nitrogen limitation) should be used rather than the realized ones ($V_{cmax25}$ already with nitrogen limitation). Therefore, in this study, to improve the representation of $V_{cmax}$ in CLM4.5 and its performance in terrestrial carbon cycle simulation, we revise the original $V_{cmax}$ scheme in CLM4.5-CN with a new one that simply accounts for the transition between $V_{cmax25}$ and $V_{cmax25}^{opt}$. Comparisons of simulated GPP, NPP, and LAI using CLM4.5-CN with the two different $V_{cmax25}$ schemes are presented to validate the model's performance.

## 2 Methods

### 2.1 Model description and improvement

CLM4.5 is the latest version of the CLM model family and is the land component of version 1.2 of the Community Earth System Model (Oleson et al., 2013). It succeeds CLM4 with updates to photosynthesis, soil biogeochemistry, fire dynamics, cold region hydrology, the lake model, and the biogenic volatile organic compounds model (Li et al., 2014). The resulting model is fully prognostic with respect to all water, energy, carbon, and nitrogen variables in the terrestrial ecosystem (Oleson et al., 2013). A detailed description of its biogeophysical and

*Corresponding author: XIE Zheng-Hui, zxie@lasg.iap.ac.cn

biogeochemical parameterizations and numerical implementation is given in Oleson et al. (2013).

CLM4 and CLM4.5 can both be run with or without an active CN. When CN is active, i.e., nitrogen limitation is prognostic, potential GPP is calculated from the leaf photosynthetic rate without nitrogen constraint. The nitrogen required to achieve this potential GPP is then diagnosed, and the actual GPP is decreased if there is insufficient nitrogen to maintain the potential biomass increment. The nitrogen inducing the reduction of GPP is applied after the photosynthesis calculation and is independent of $V_{cmax}$, but does implicitly decrease $V_{cmax}$ (Bonan et al., 2011, 2012). When CN is inactive, i.e., nitrogen limitation is prescribed, the potential $V_{cmax25}^{opt}$ is directly reduced by multiplying a prescribed nitrogen limitation factor $f$(N):

$$V_{cmax25} = V_{cmax25}^{opt} \times f(\mathrm{N}), \quad (1)$$

where $f$(N) is scaled between zero and one so that GPP is similarly decreased for nitrogen availability.

In CLM4.5, the original potential $V_{cmax25}^{opt}$ used in CLM4, specified for each plant functional type (PFT) in the absence of nitrogen limitation (Thornton and Zimmermann, 2007), is replaced with $V_{cmax25}^{kattge}$ (Bonan et al., 2012); and to make this meaningful, PFT-specific values for $f$(N) in CLM4 (denoted as $f_2$(N)) for runs without CN, were all changed to 1 in CLM4.5 (denoted as $f_1$(N)). However, when CN is active, CLM4.5 still uses $V_{cmax25}^{kattge}$ as the potential $V_{cmax25}^{opt}$ values for the calculation of GPP. Unfortunately, this may cause double nitrogen down-regulation. Therefore, to address this problem, we still use $f_2$(N) as the explicit nitrogen limitation factor in CLM4.5 and divide the $V_{cmax25}^{kattge}$ values, which already reflect nitrogen via $f_2$(N) (like Eq. (2)), to obtain the potential values of $V_{cmax25}^{opt}$ that match with $V_{cmax25}^{kattge}$. Those values for $V_{cmax25}^{kattge}$, $f_1$(N), $f_2$(N), and $V_{cmax25}^{opt}$ are all listed in Table 1. The revision makes no difference to the calculation of GPP when CN is inactive, but does when CN is active.

$$V_{cmax25}^{opt} = V_{cmax25}^{kattge} / f_2(\mathrm{N}). \quad (2)$$

## 2.2 Data

### 2.2.1 Land cover data

An accurate land cover map can significantly reduce the uncertainty of land surface modeling. Based on Dempster-Shafer evidence theory, Ran et al. (2012) developed a high-accuracy (1 km) multi-source integrated Chinese land cover dataset (MICLCover), which shows great improvement compared to other popular land cover maps. It was generated using the International Geosphere Biosphere Programme classification system by combining five sets of relevant land cover data: the Vegetation Atlas of China (1:1 000 000) (Hou, 2001); a land use map of China (1:100 000) for the year 2000 (Liu et al., 2002); a glacier distribution map of China (1:100 000) (Wu and Li, 2004); a swamp-wetland map of China (1:1 000 000) (Zhang, 2002); and the Moderate Resolution Imaging Spectroradiometer (MODIS) product for 2001 (MODIS2001) (Friedl et al., 2002). The MICLCover map (http://westdc.westgis.ac.cn/dat) is expressed by the percentages of glaciers, lakes, wetland, urban land, and 16 PFTs in each grid, consistent with the classification in CLM. Yu et al. (2014) and Wang et al. (2015) found that the MICLCover map has the potential to improve land surface modeling with CLM. Here, we upscale the MICLCover map from 1 km to 0.5° by means of an area-weighted average and use it as the land cover data in CLM4.5 (Wang et al., 2015).

**Table 1** PFT (plant functional type)-specific photosynthetic parameters. $V_{cmax25}^{kattge}$ is the realized $V_{cmax25}$ values obtained from Kattge et al. (2009); $f_1$(N) is the prescribed nitrogen limitation factor used in CLM4.5, while $f_2$(N) is from CLM4.0; and $V_{cmax25}^{opt}$, which represents the potential values for $V_{cmax25}$, is given by $V_{cmax25}^{opt} = V_{cmax25}^{kattge} / f_2(\mathrm{N})$.

| Plant functional type | $V_{cmax25}^{kattge}$ | $f_1$(N) | $f_2$(N) | $V_{cmax25}^{opt}$ |
|---|---|---|---|---|
| Needleleaf evergreen tree, temperate | 62.5 | 1 | 0.72 | 86.8 |
| Needleleaf evergreen tree, boreal | 62.6 | 1 | 0.78 | 80.2 |
| Needleleaf deciduous tree, boreal | 39.1 | 1 | 0.79 | 49.5 |
| Broadleaf evergreen tree, tropical | 55.0 | 1 | 0.83 | 66.3 |
| Broadleaf evergreen tree, temperate | 61.5 | 1 | 0.71 | 86.8 |
| Broadleaf deciduous tree, tropical | 41.0 | 1 | 0.66 | 62.1 |
| Broadleaf deciduous tree, temperate | 57.7 | 1 | 0.64 | 90.1 |
| Broadleaf deciduous tree, boreal | 57.7 | 1 | 0.70 | 82.4 |
| Broadleaf evergreen shrub, temperate | 61.7 | 1 | 0.62 | 99.5 |
| Broadleaf deciduous shrub, temperate | 54.0 | 1 | 0.60 | 90.0 |
| Broadleaf deciduous shrub, boreal | 54.0 | 1 | 0.76 | 71.0 |
| C3 grass, arctic | 78.2 | 1 | 0.68 | 115.0 |
| C3 grass | 78.2 | 1 | 0.61 | 128.1 |
| C4 grass | 51.6 | 1 | 0.64 | 80.6 |
| Crop | 100.7 | 1 | 0.61 | 165.1 |

### 2.2.2 Atmospheric forcing data

To run CLM in the offline mode, atmospheric forcing data are required. The standard forcing provided with the model is a half-degree 110-year (1901–2010) dataset (CRUNCEP; Viovy, 2011) that includes precipitation, incident solar radiation, temperature, pressure, winds, humidity, and incident longwave radiation. It is a combination of two existing datasets: version 3.2 of the Climate Research Unit Time Series (CRU TS3.2) 0.5° × 0.5° monthly data from 1901 to 2002, and the National Centers for Environmental Prediction (NCEP) reanalysis 2.5° × 2.5° six-hourly data from 1948 to 2010 (Oleson et al., 2013).

### 2.2.3 Observation data

Three products are used for benchmarking our comparisons: the global GPP (monthly, 0.5° × 0.5°), upscaled from FLUXNET observations using the machine learning technique, model tree ensembles (MTE) from 1982 to 2011 (Jung et al., 2009, 2011, denoted as MTE_GPP); the global MODIS NPP product (MODIS17A2, monthly, 0.5° ×

0.5°, denoted as MODIS_NPP) from 2000 to 2013; and the MODIS LAI product (MODIS15A2, monthly, 0.5° × 0.5°, denoted as MODIS_LAI) from 2000 to 2013. The MODIS LAI and NPP data are obtained from NASA Earth Observations (http://neo.sci.gsfc.nasa.gov/).

### 2.3 Experimental design

To investigate the effect of the revised $V_{cmax}$ scheme on terrestrial carbon cycle modeling, two experiments using CLM4.5-CN were conducted with 0.5° × 0.5° resolution using the 20-year (1991–2010) CRUNCEP datasets as atmospheric forcing data and MICLCover map as surface data: (1) a control run with the default $V_{cmax}$ scheme (denoted as CTL); (2) a new run with the revised $V_{cmax}$ scheme (denoted as NEW). Besides the difference in the $V_{cmax}$ schemes of the two experiments, all the other model configurations and input data were exactly the same. Both experiments were spun up for 1500 years for establishing the carbon and nitrogen pools and fluxes (Hudiburg et al., 2013; Kendra et al., 2012), forced circularly by 20 years' atmospheric forcing. Subsequently, two simulations from 2000 to 2010 are analyzed.

To evaluate the model's performance, GPP, NPP, and LAI, which are the dominant components of the terrestrial carbon cycle from the two runs, are analyzed (denoted as CTL_GPP, CTL_NPP, and CTL_LAI, and NEW_GPP, NEW_NPP, and NEW_LAI, respectively). For time consistency, the simulated annual means of GPP, NPP, and LAI from 2000 to 2010 are compared with observations over China for the same time period.

To quantify the performance of the two $V_{cmax}$ schemes in comparison with observations, we computed the correlation coefficient ($R$) and root-mean-square error (RMSE), defined as follows:

$$R = \frac{\sum_{i=1}^{N}(x_i - \overline{x})(\mathrm{obs}_i - \overline{\mathrm{obs}})}{\sqrt{\sum_{i=1}^{N}(x_i - \overline{x})^2}\sqrt{\sum_{i=1}^{N}(\mathrm{obs}_i - \overline{\mathrm{obs}})^2}}, \quad (3)$$

$$\mathrm{RMSE} = \sqrt{\frac{\sum_{i=1}^{N}(x_i - \mathrm{obs}_i)^2}{N}}, \quad (4)$$

where $x$ is the model simulation either from CTL or NEW, obs is the corresponding observation, $\overline{x}$ and $\overline{\mathrm{obs}}$ are the mean value of $x$ and obs, respectively.

## 3 Results

### 3.1 GPP

Figure 1 shows the spatial distributions of mean GPP from model simulations (CTL_GPP and NEW_GPP) and observation (MTE_GPP), together with their differences. To examine regional differences in the performance of the $V_{cmax}$ schemes, four sub-regions over China are defined according to mean annual precipitation, $P_{mean}$: arid ($P_{mean} \leqslant$ 200 mm); semi-arid (200 mm < $P_{mean}$ < 400 mm); semi-humid (400 mm < $P_{mean}$ < 800 mm); humid ($P_{mean}$ > 800 mm) (Yu et al., 2014). The spatial patterns of the simulated GPP are very similar (Figs. 1a and 1b), being characterized by a southeast-northwest gradient, consistent with MTE_GPP (Fig. 1c), with the largest annual GPP in humid regions, followed by semi-humid regions, semi-arid regions, and arid regions. The GPP annual means of the two simulations in China are 8.17 and 7.85 Pg C yr$^{-1}$ respectively, which are much higher than the 7.05 Pg C yr$^{-1}$ of MTE_GPP, albeit with obvious reduction in NEW_GPP. Although both simulations overestimate GPP in humid areas (Figs. 1d and 1e), NEW_GPP shows large improvements in these areas with a mean reduction of −65.4 g C m$^{-2}$ yr$^{-1}$. Apart from in the arid regions dominated by C3 or C4 grass and bare areas (not shown), the values of GPP are reduced significantly at the 95% confidence level in Qinghai-Tibet and southwest areas, which are dominated by cropland and trees (Fig. 1f). Although the values of new $V_{cmax}$ are higher than the original values, which may induce higher potential leaf photosynthetic rates, the reduced total soil water availability ($\beta_t$) and nitrogen availability ($f_N$) of the NEW run (not shown) decrease the GPP simulation, achieved by multiplying $V_{cmax}$ by $\beta_t$ and GPP by $f_N$, respectively. The scatterplots between the simulated GPP, NPP, LAI and observations and the MTE_GPP are shown in Fig. 3. The RMSE for the CTL_GPP for the whole of China is 360.8 g C m$^{-2}$ yr$^{-1}$, whereas the NEW_GPP reduces the RMSE by 13.7 g C m$^{-2}$ yr$^{-1}$, though the new $V_{cmax}$ has little effect on the spatial correlation between the simulated GPP and MTE_GPP. Although the new $V_{cmax}$ further underestimates mean annual GPP in semi-humid and semi-arid regions, there are improvements in the other areas, with lower RMSEs (Fig. 4b), more obvious in humid regions, where the RMSE is reduced from 622.5 to 583.2 g C m$^{-2}$ yr$^{-1}$.

### 3.2 NPP

Figure 1 also shows the spatial patterns of mean NPP. It can be seen that the CTL and NEW model simulations and observations (MODIS_NPP) show broadly similar patterns, with a northwest-southeast gradient over China (Figs. 1g–i). Compared with MODIS observations, CLM4.5 simulations clearly overestimate NPP in most areas of China, especially humid areas (Figs. 1j and 1k). The NPP means over China for CTL, NEW, and MODIS are 3.81, 3.78, and 2.71 Pg C yr$^{-1}$, respectively. The scatterplots between CLM4.5 simulations and MODIS observations show that the new $V_{cmax}$ scheme reduces the RMSE from 260.9 (CTL) to 260.7 g C m$^{-2}$ yr$^{-1}$. The mean annual NPP of the NEW run shows improvements in all four sub-regions compared to MODIS_NPP, with an increase of 0.7 g C m$^{-2}$ yr$^{-1}$ in arid areas and decreases of 8.3, 8.7, and 4.1 g C m$^{-2}$ yr$^{-1}$ in semi-arid, semi-humid, and humid areas, respectively. Furthermore, the RMSEs of NPP for the four sub-regions from the NEW run are all lower than those from the CTL run, especially for semi-arid and semi-humid areas, which also reflect the success of the revised $V_{cmax}$ scheme (Fig. 4d).

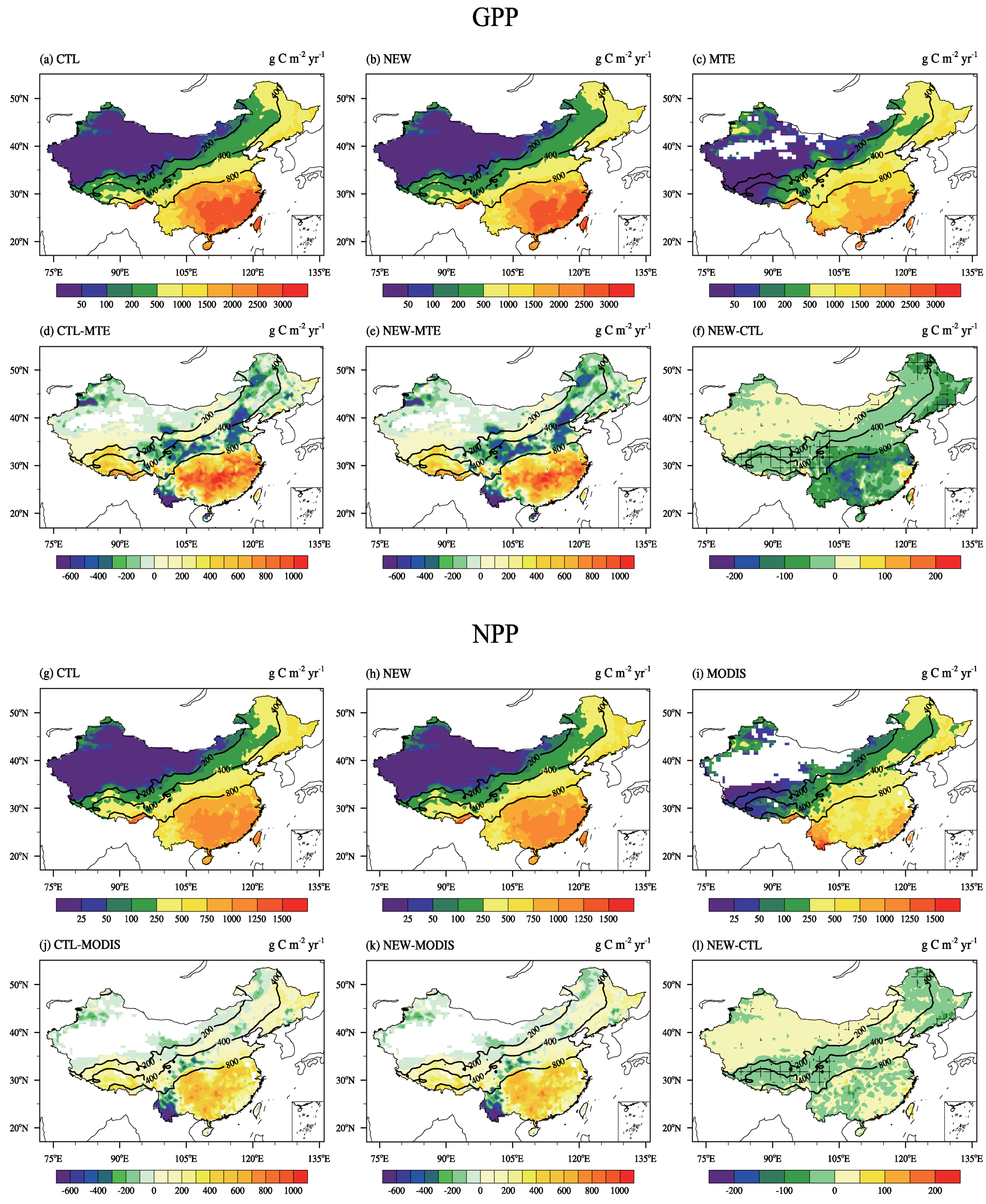


**Figure 1** Eleven-year (2000–10) mean gross primary production (GPP) from the (a) control run (CTL_GPP), (b) new $V_{\rm cmax}$ scheme (NEW_GPP), (c) observations (MTE_GPP), (d) CTL_GPP minus MTE_GPP, (e) NEW_GPP minus MTE_GPP, and (f) NEW_GPP minus CTL_GPP. Panels (g–l) are the same as GPP but for net primary production (NPP) from (g) CTL_NPP, (h) NEW_NPP, (i) MODIS_NPP, (j) CTL_NPP minus MODIS_NPP, (k) NEW_NPP minus MODIS_NPP, and (l) NEW_NPP minus CTL_NPP. The grid shadow regions are significant at the 95% confidence level by student's $t$ test, and the isolines refer to the mean annual precipitation (mm yr$^{-1}$).

### 3.3 LAI

Figure 2 shows the spatial distributions of mean annual LAI from MODIS and the two CLM4.5 simulations and their differences. It is found that, as with GPP and NPP, the simulated LAI and MODIS_LAI all show southeast-northwest gradient (Figs. 2a–c). Both LAI simulations have positive biases in almost all areas of China, especially humid areas (Figs. 2d and 2e). However, the revised $V_{\rm cmax}$ scheme causes reductions in LAI in semi-arid, semi-humid, and humid areas (Fig. 2f), resulting in lower RMSE (2.3) in China compared with those of CTL_LAI (RMSE = 2.6) (Figs. 3e and 3f). And just like

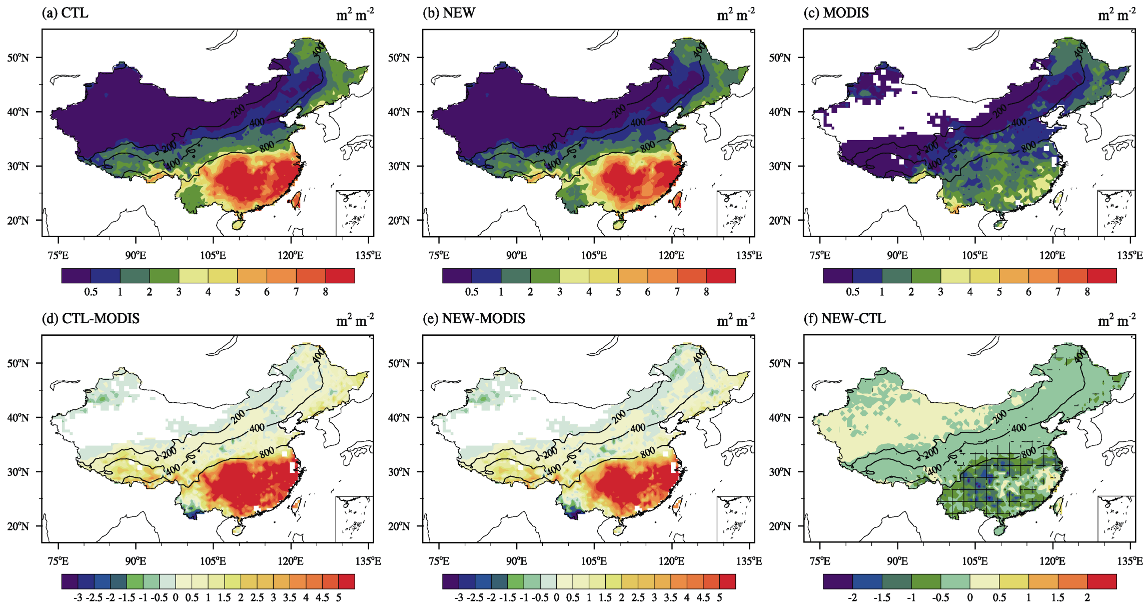


**Figure 2** Eleven-year (2000–10) mean leaf area index (LAI) from the (a) control run (CTL_LAI), (b) new $V_{\mathrm{cmax}}$ scheme (NEW_LAI), (c) observations (MODIS_LAI), (d) CTL_LAI minus MODIS_LAI, (e) NEW_LAI minus MODIS_LAI, and (f) NEW_LAI minus CTL_LAI. The grid shadow regions are significant at the 95% confidence level by student's $t$ test, and the isolines refer to the mean annual precipitation (mm yr$^{-1}$).

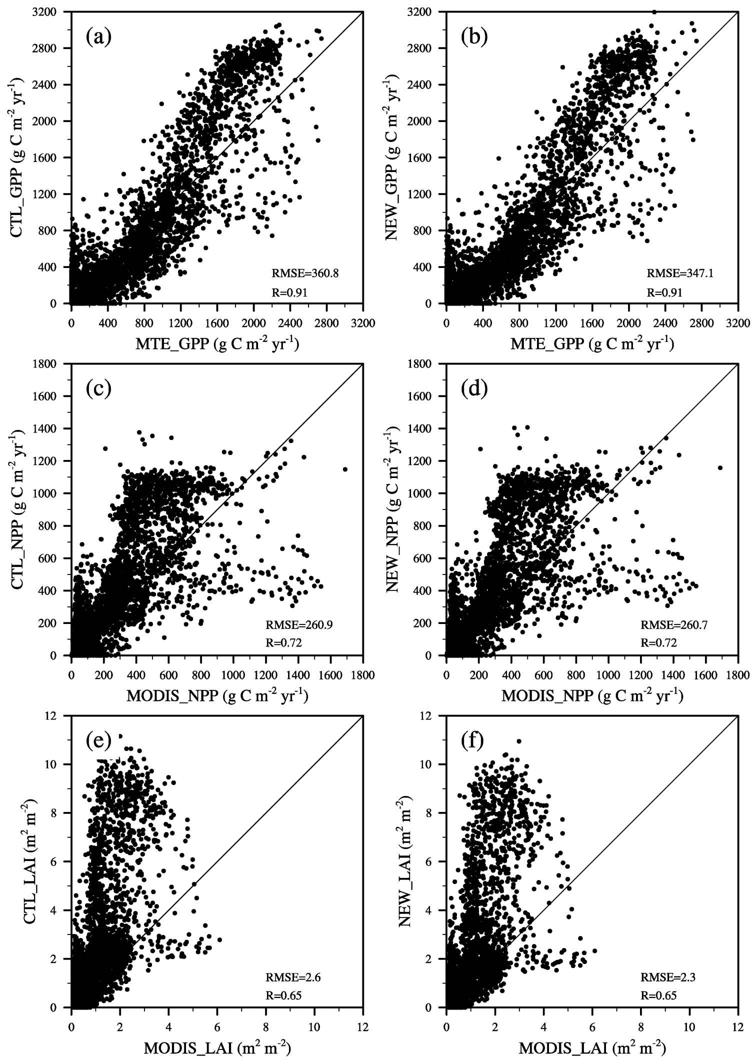


**Figure 3** Comparison of annual GPP, NPP, and LAI from CLM4.5 model simulations (CTL and NEW) on 0.5° collocated grid boxes, with the corresponding observational data. RMSE = root-mean-square error; $R$ = correlation coefficient.

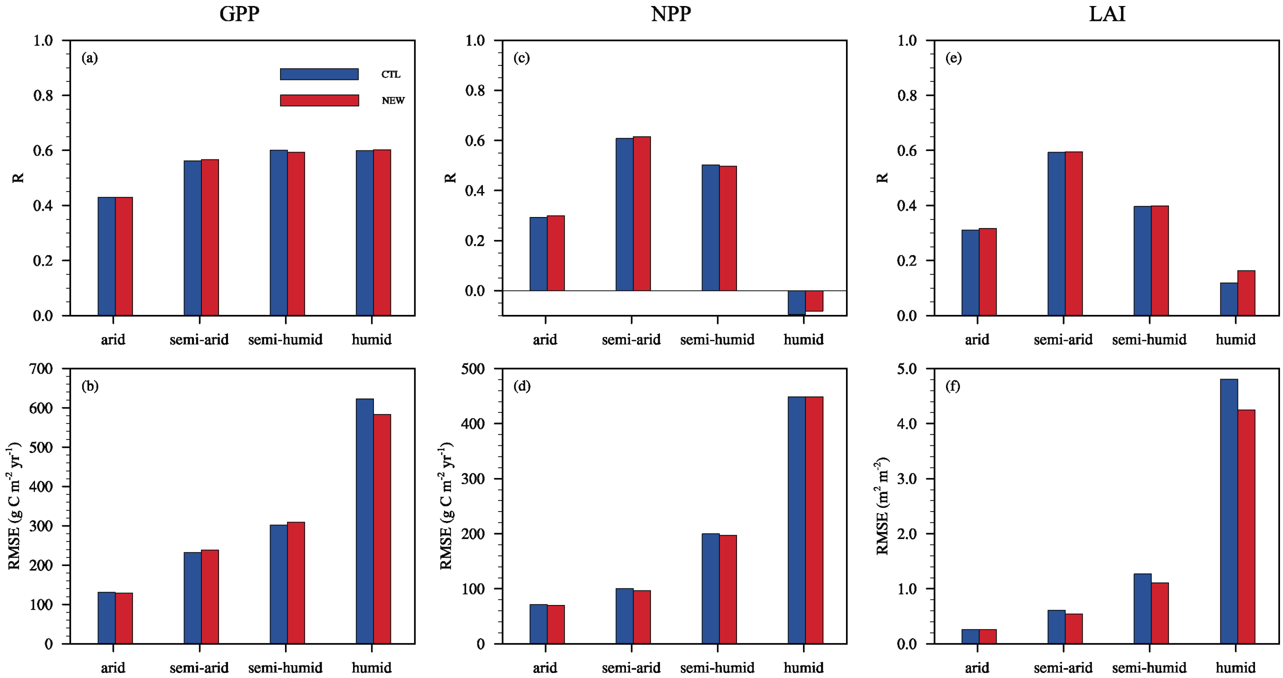


**Figure 4** Comparison results of the control run (CTL) and new scheme (NEW) for (a–b) GPP, (c–d) NPP, and (e–f) LAI compared with observations over the four sub-regions: arid, semi-arid, semi-humid, and humid.

NPP, the RMSEs of LAI for the four sub-regions from NEW are all notably decreased, especially for humid areas, where RMSE is decreased from 4.8 to 4.2 (Fig. 4f).

## 4 Conclusion and discussion

As a key parameter for GPP simulation, $V_{cmax}$ is required to be as accurate as possible in land surface models. In this study, to avoid the double nitrogen reduction of GPP in CLM4.5-CN, we revise the original $V_{cmax}$ scheme with a new one that simply considers the transition between $V_{cmax25}$ and $V_{cmax25}^{opt}$, and implement it into CLM4.5-CN. By comparison, we find that the revised $V_{cmax}$ can reduce the RMSEs of simulated GPP for the whole of China, arid areas, and humid areas by 13.7, 1.4, and 39.2 g C m$^{-2}$ yr$^{-1}$, respectively. And similar improvements are seen for RMSEs. Although the new scheme has higher $V_{cmax}$ values compared with the original one, which may induce higher potential leaf photosynthetic rates, the reduced soil water availability and nitrogen availability of the NEW run decrease the GPP estimation in CLM4.5-CN. This indicates that change in $V_{cmax}$ might have multiple impacts on photosynthesis, through the complicated interactions between photosynthesis, respiration, soil moisture, and the soil nitrogen pool, which needs further study. For NPP and LAI, the RMSEs for the whole of China and the four sub-regions from the NEW run are all lower than those from the CTL run. The greatest improvements of NPP are in semi-arid and semi-humid areas, with reductions of RMSE by 3.7 and 2.7 g C m$^{-2}$ yr$^{-1}$, respectively. The RMSE of LAI in humid areas is also obviously reduced, from 4.8 to 4.2. Additionally, for both the seasonal cycle and interannual variations, GPP, NPP, and LAI simulated by the NEW run also show great improvements in arid and humid areas, with reduced RMSEs (not shown). Overall, the new $V_{cmax}$ scheme can improve the terrestrial carbon cycle modeling of CLM4.5-CN.

$V_{cmax}$ values of most terrestrial biosphere models are PFT-specific, including CLM4.5. However, some studies show that $V_{cmax}$ may vary greatly even within a PFT, so a simple classification of photosynthesis parameters such as $V_{cmax}$ may introduce large uncertainty (Bonan et al., 2011; Hudiburg et al., 2013). Therefore, a refinement of $V_{cmax}$ parameter estimation is needed for CLM4.5 and other terrestrial biosphere models in future work.

**Acknowledgements.** This study was supported by the National Natural Science Foundation of China (Grant Nos. 91125016 and 41305066) and the Strategic Priority Research Program of the Chinese Academy of Sciences (Grant No. XDA05110102).

## References

Bonan, G. B., P. J. Lawrence, K. W. Oleson, et al., 2011: Improving canopy processes in the Community Land Model version 4 (CLM4) using global flux fields empirically inferred from FLUXNET data, *J. Geophys. Res.*, **116**, G02014, doi:10.1029/2010JG001593.

Bonan, G. B., K. W. Oleson, R. A. Fisher, et al., 2012: Reconciling leaf physiological traits and canopy flux data: Use of the TRY and FLUXNET databases in the Community Land Model version 4, *J. Geophys. Res.*, **117**, G02026, doi:10.1029/2011JG001913.

Chen, H. S., R. E. Dickinson, Y. J. Dai, et al., 2011: Sensitivity of simulated terrestrial carbon assimilation and canopy transpiration to different stomatal conductance and carbon assimilation schemes, *Climate Dyn.*, **36**, 1037–1054.

Collatz, G. J., J. T. Ball, C. Grivet, et al., 1991: Physiological and environmental regulation of stomatal conductance, photosynthesis and transpiration: A model that includes a laminar boundary layer, *Agric. Forest Meteor.*, **54**, 107–136.

Farquhar, G. D., S. von Caemmerer, and J. A. Berry, 1980: A biochemical model of photosynthetic $CO_2$ assimilation in leaves of C3 species, *Planta*, **149**, 78–90.

Friedl, M. A., D. K. McIver, J. C. F. Hodges, et al., 2002: Global land cover mapping from MODIS: Algorithms and early results, *Remote Sens. Environ.*, **83**(1–2), 287–302.

Hou, X. Y., 2001: *Vegetation Atlas (1:1,000,000) of China* (in Chinese), Sciences Press, Beijing, 260pp.

Hudiburg, T. W., B. E. Law, and P. E. Thornton, 2013: Evaluation and improvement of the Community Land Model (CLM4) in Oregon forests, *Biogeosciences*, **10**, 453–470.

Jung, M., M. Reichstein, and A. Bondeau, 2009: Towards global empirical upscaling of FLUXNET eddy covariance observations: Validation of a model tree ensemble approach using a biosphere model, *Biogeosciences*, **6**, 2001–2013.

Jung, M., M. Reichstein, H. A. Margolis, et al., 2011: Global patterns of land-atmosphere fluxes of carbon dioxide, latent heat, and sensible heat derived from eddy covariance, satellite, and meteorological observations, *J. Geophys. Res.*, **116**, G00J07, doi:10.1029/2010JG001566.

Kattge, J., S. Díaz, S. Lavorel, et al., 2011: TRY: A global database of plant traits, *Glob. Change Biol.*, **17**, 2905–2935, doi:10.1111/j.1365-2486.2011.02451.x.

Kattge, J., W. Knorr, T. Raddatz, et al., 2009: Quantifying photosynthetic capacity and its relationship to leaf nitrogen content for global scale terrestrial biosphere models, *Glob. Change Biol*., **15**, 976–991.

Kendra G. C., C., S. Levis, and P. Thornton, 2012: Evaluation of the new CNDV option of the Community Land Model: Effects of dynamic vegetation and interactive nitrogen on CLM4: Means and variability, *J. Climate*, **25**, 3702–3714.

Li, F., B. Lamberty, and S. Levis, 2014: Quantifying the role of fire in the Earth system—Part 2: Impact on the net carbon balance of global terrestrial ecosystems for the 20th century, *Biogeosciences*, **11**, 1345–1360.

Liu, J. Y., M. L. Liu, X. Z. Deng, et al., 2002: The land use and land cover change database and its relative studies in China, *J. Geogr. Sci.*, **12**(3), 275–282.

Oleson, K. W, D. M. Lawrence, G. Bonan, et al., 2013: *Technical Description of Version 4.5 of the Community Land Model (CLM)*, NCAR Tech. Note, NCAR/TN-503+STR, 434pp.

Ran, Y. H., X. Li, L. Lu, et al., 2012: Large-scale land cover mapping with the integration of multi-source information based on the Dempster-Shafer theory, *Int. J. Geogr. Inf. Sci.*, **26**(1), 169–191.

Schaefer, K., C. R. Schwalm, C. Williams, et al., 2012: A model-data comparison of gross primary productivity: Results from the North American Carbon Program site synthesis, *J. Geophys. Res.*, **117**, G03010, doi:10.1029/2012JG001960.

Thornton, P. E., and N. E. Zimmermann, 2007: An improved canopy integration scheme for a land surface model with prognostic canopy structure, *J. Climate*, **20**, 3902–3923.

Viovy, N., 2011: *CRUNCEP Dataset*, description available at http://dods.extra.cea.fr/data/p529viov/cruncep/readme.htm, data available at http://dods.extra.cea.fr/store/p529viov/cruncep/V4_1901_2011/.

Wang, Y. Y., Z. H. Xie, B. H. Jia, et al., 2015: Simulation and evaluation of the gross primary productivity in China using the land surface model CLM4, *Climatic Environ. Res.*, **20**(1), 97–110.

Wu, L., and X. Li, 2004: *China Glacier Information System* (in Chinese), Ocean Press, Beijing, 1–135.

Yu, Y., Z. H. Xie, Y. Y. Wang, et al., 2014: Results of a CLM4 land surface simulation over China using a multisource integrated land cover dataset, *Atmos. Oceanic. Sci. Lett.*, **7**, 279–285.

Zhang, S., 2002: An introduction of wetland science database in China, *Sci. Geogr. Sinica* (in Chinese), **22**(2), 188–189.